Supplementary Figures

**Figure S1.** Aldosterone, potassium and sodium in bodily fluids. (**A**) Summary graph comparing serum aldosterone levels in SHR-B2 (black) and SHR-A3 (grey). (**B**) Summary graph comparing potassium to creatinine ratio in spot urine samples from SHR-B2 and SHR-A3. (**C**) Summary graph demonstrating averaged serum potassium levels in SHR-B2 and SHR-A3. (**D**) Summary graph showing sodium to creatinine ratio in spot urine samples from SHR-B2 and SHR-A3. (**E**) Summary graph comparing average serum sodium concentrations in SHR-A3 and SHR-B2. * – P < 0.05 versus SHR-B2, estimated with one-way ANOVA test. The number of animals in each group is indicated on top of the respective bars.
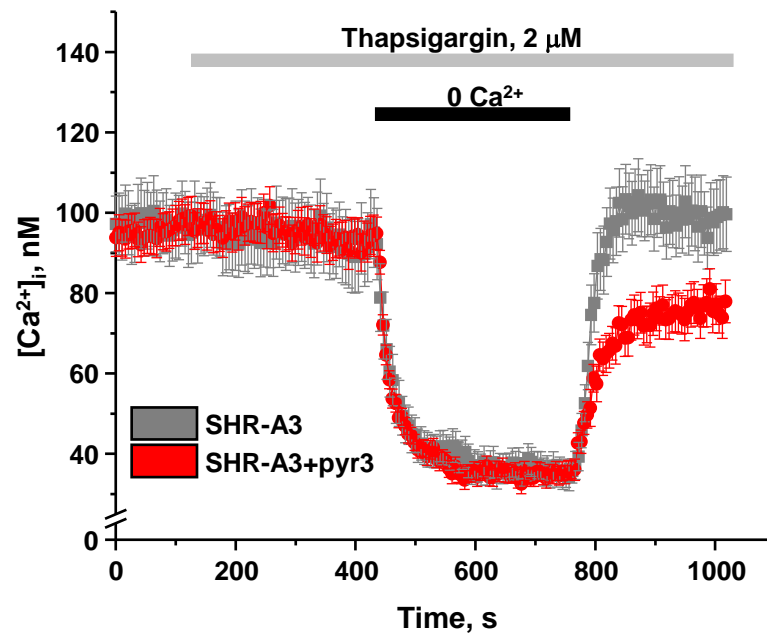
Figure S2. The average time courses of $[Ca^{2+}]_i$ changes in response to Ca^{2+} removal – Ca^{2+} re-addition protocol upon depletion of $[Ca^{2+}]_i$ stores with thapsigargin recorded in CD cells from SHR-A3 in the control (grey) and on the background of nonspecific TRPC3/ORAI1 inhibitor – pyr3 (5 µM, shown in red).
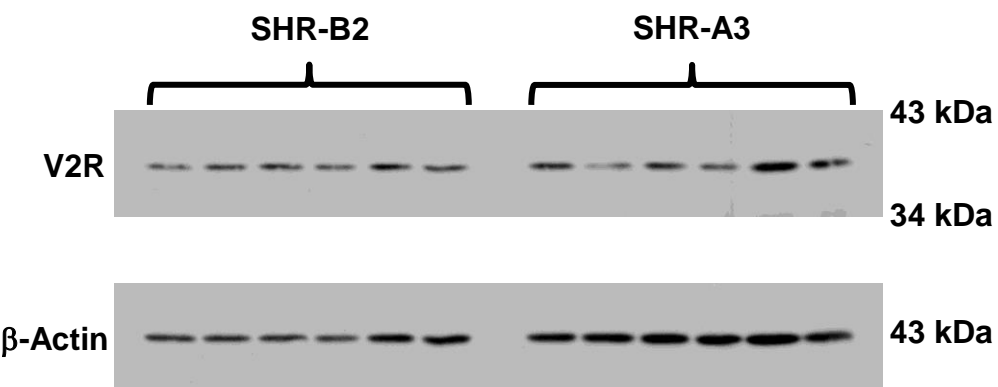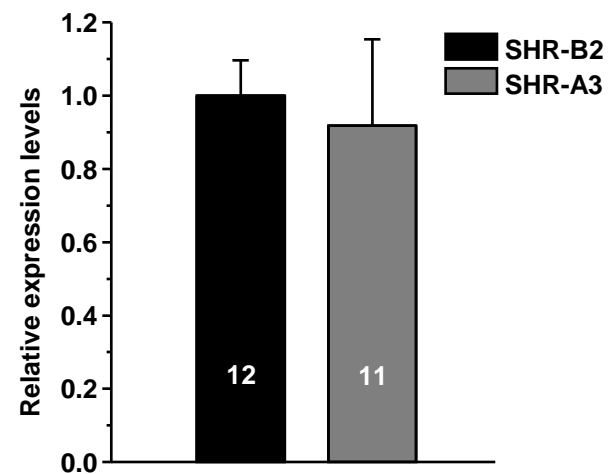
Figure S3. (**A**) Representative western blot from whole kidney lysates of SHR-B2 and SHR-A3 probed with anti-V2R and anti-b-actin antibodies. (**B**) Summary graph comparing total renal V2R expression in SHR-B2 (black) and SHR-A3 (grey) from western blots similar to that shown in (A). The number of animals in each group is indicated on top of the respective bars.

A.
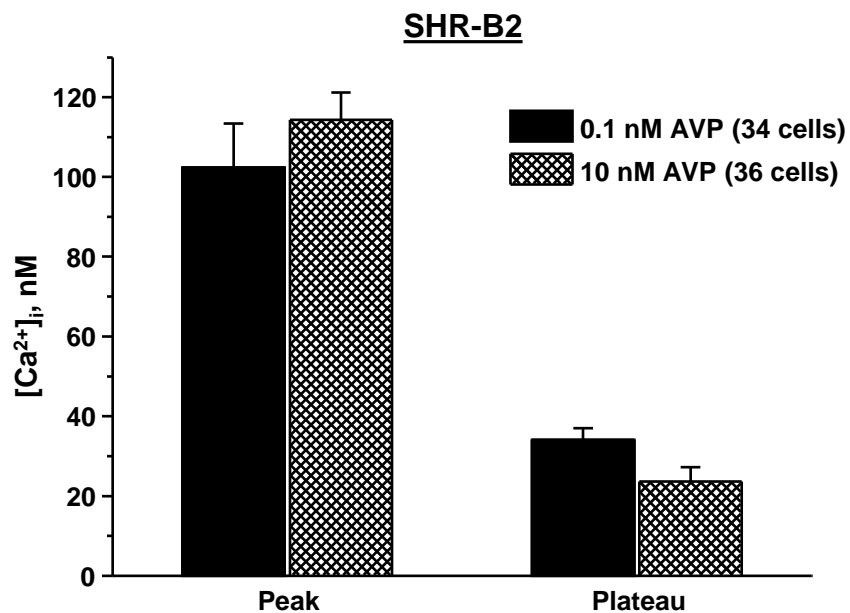
B.
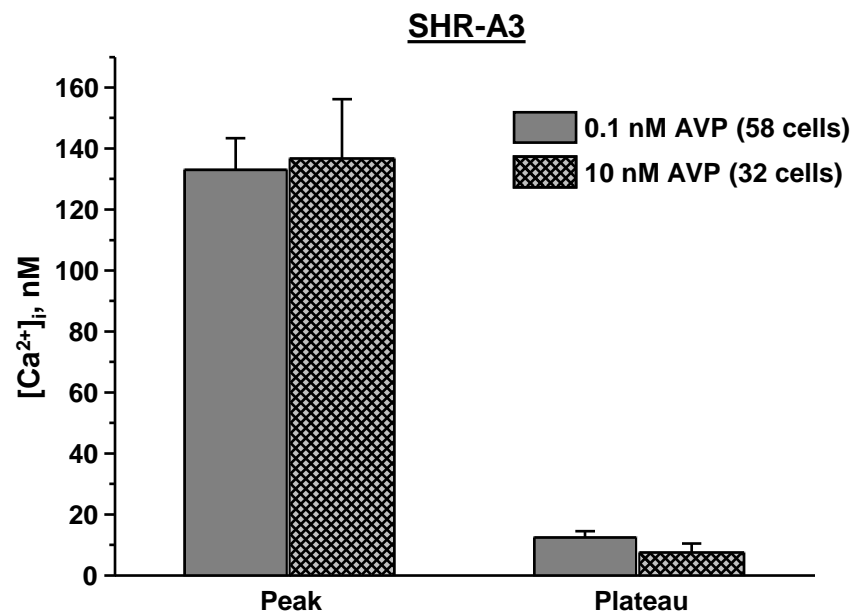
Figure S4. Summary graphs comparing the average magnitudes of transient peak (left panels) and sustained plateau (right panels) phases of [Ca^{2+}]$_i$ responses recorded in CD cells from SHR-B2 (**A**) and SHR-A3 (**B**) upon treatment 0.1 nM and 10 nM of AVP. The number of cells in each treatment group is indicated near respective figure legend bars.
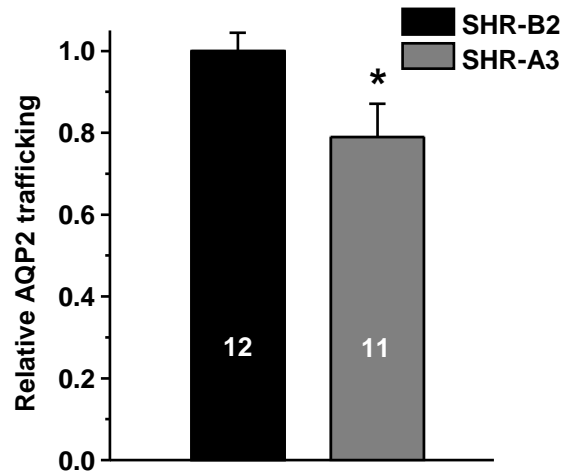
Figure S5. Summary graph comparing estimated relative rates of AQP2 trafficking in SHR-B2 (black) and SHR-A3 (gray). * – P < 0.05 versus SHR-B2, estimated with one-way ANOVA test. The number of animals in each group is indicated on top of the respective bars.